TASK QUARTERLY 5 No 1 (2001), 99–107

HEAT TRANSFER ANALYSIS FOR THE HYDRAULIC CIRCUIT OF AN EXPRESSO-COFFEE MACHINE

LAURO FIORETTI[1] AND MASSIMO CONTI[2]

[1]*Nuova Simonelli,*
Via Madonna d'Antenagio 62-031 Belforte (MC), Italy
fioretti@nuovasimonelli.it

[2]*Dipartimento di Matematica e Fisica,*
Università di Camerino,
Madonna delle Carceri, I-62032 Camerino, Italy
conti@campus.unicam.it

(Received 4 December 2000)

Abstract: An Espresso-Coffee Machine supplies water whose temperature must be confined within a narrow range in different operating conditions; this requires an accurate design at the component as well as the system level. In the present paper we develop a mathematical model to analyse the performances of the heating circuit of such a machine; our aim is to capture the main operating characteristics of the system with the maximum of simplicity. The governing equations of the model have been solved with the finite difference technique, and the first results have been compared with some experimental data.

Keywords: heat transfer

1. Introduction

The taste and the flavour of a well made espresso coffee represent a central issue in several countries and civilizations. The know-how which underlies this problem has been considered for some time an artistic talent belonging to few esoteric people. When it became clear that the pleasure of good coffee could not be confined within the borders of some regions of Italy, it was necessary to identify in a more objective way the secrets of this art. Then, studies were promoted in two main directions: the chemical and physical processes which occur when the hot water percolates along the coffee filter, and the optimization of the thermal design of an Espresso-Coffee Machine (ECM) which operates in very different load conditions. This latter point is the subject of the present paper.

Schematically, an ECM injects hot water into the coffee filter; for best result the water temperature must be confined within a narrow range around 90°C. The water demand alternates from active phases (corresponding to the coffee percolation) to idle phases (no coffee delivery). It should be noted that the duration of the idle phases is not predictable a priori. The system should meet the requirements of low cost and high reliability; in

this perspective in most of the commercial machines the use of sophisticated sensors and actuators has been avoided.

In the following workwe present a mathematical model which simulates the thermo-hydraulic behaviour of the heating circuit of such a machine. Our aim is to set up a simple tool which captures the main operating characteristics of the system with the maximum of simplicity, in order to attempt the optimization of the machine both at the system and at the components level. The model equations have been discretized and solved with the finite difference method. First numerical results indicate good agreement between the model predictions and the experimental data.

2. The hydraulic circuit and the model equations

2.1. The layout of the hydraulic circuit

The heating circuit of the coffee machine is described in Figure 1, where the arrows indicate the flow diagram for the active phase. A bayonet heat exchanger, tilted with an angle $\gamma = \pi/4$ on the horizontal plane, is immersed in a boiler containing pressurized water ad vapour at fixed temperature $T_B = 120^{\circ}\mathrm{C}$. During the active phase of the cycle the valves V1 and V2 are open. Water at temperature T_i is supplied to the inlet of the heat exchanger where it is heated and transferred, through the two independent channels C1 and C2, to a mixer M whose massive walls act as a heat storage system. Then the water is delivered to the coffee percolator. The flow diagram for the idle phase of the cycle is indicated in Figure 2. Now the valves V1 and V2 are closed and the water supply to and from the circuit is interrupted. Then, a natural flow is activated, due to the thermal gradients along the hydraulic path. The nozzle J1 regulates the total flow rate during the idle phase, and the relative flow in the channels C1 and C2 during the active phase. To better clarify the subsequent analysis it is convenient to distinguish in the circuit 9 different elements, enumerated below (see also Figure 1).

1. The internal duct of the bayonet heat exchanger.
2. The annular region of the heat exchanger.
3. The clearance volume of the heat exchanger.
4. The outlet duct from the annular region of the heat exchanger.
5. The outlet duct from the clearance volume of the heat exchanger.
6. The continuation of duct (4) inside the mixer.
7. The continuation of duct (5) inside the mixer.
8. The outlet duct from the mixer.
9. The connection between the annular region and the duct (4).

In each element the position is indicated through an axial coordinate x defined as increasing along the flow during the active phase, except for elements 2 and 9 where x decreases along the flow. The geometrical parameters which characterize the elements of the hydraulic circuit are defined in Table 1.

Due to the tilt on the horizontal plane of the circuit elements, the axial symmetry of the problem is broken. This effect will be neglected in the following, and the thermal field will be assumed as independent of the azimuthal coordinate. Moreover, the fluid temperature along a cross section of the flow will be represented through a single value, averaged over the radial coordinate. This method allows to utilize well established thermohydraulic correlations to describe the heat transfer between the ducts walls and the fluid. Then, the

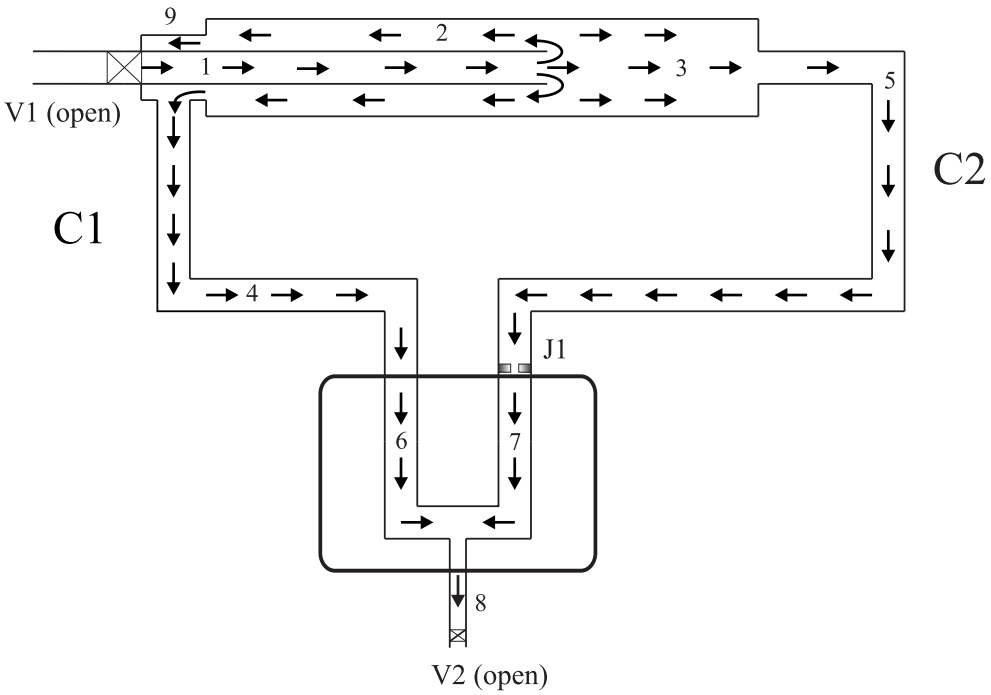

Figure 1. The layout of the heating circuit, indicating the flow diagram during the active phase

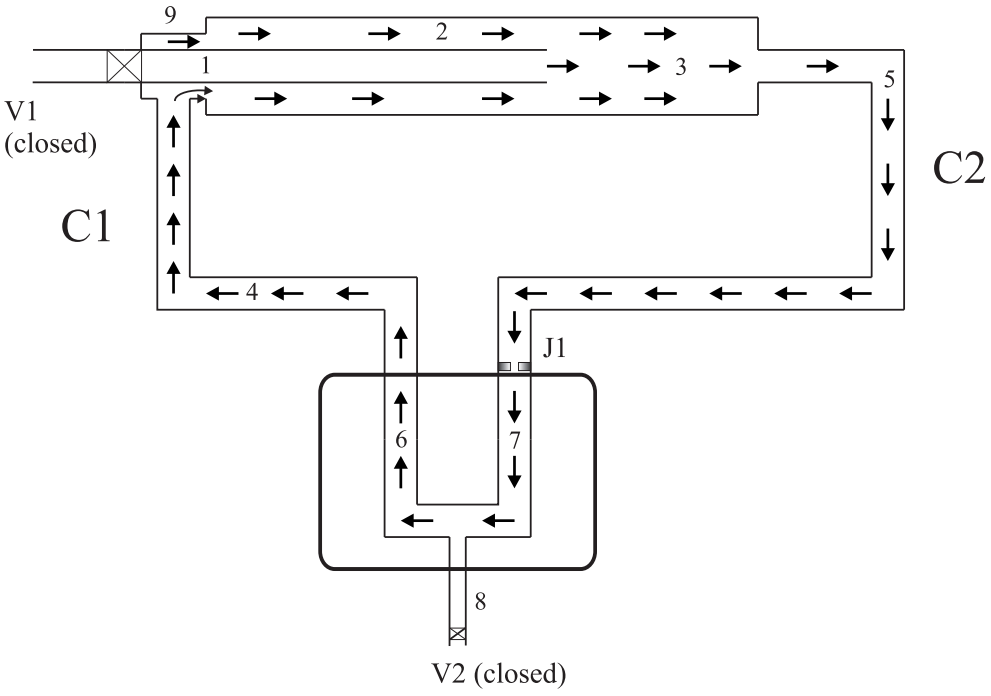

Figure 2. The layout of the heating circuit indicating the flow diagram during the idle phase

Table 1. The geometrical parameters which characterize the heating circuit

$D_{i,\mathrm{n}}(n=1\ldots9)$	Internal diameter of the duct (n)
$D_{e,\mathrm{n}}(n=1\ldots9)$	External diameter of the duct (n)
$S_{\mathrm{n}}(n=1\ldots9)$	Flow cross section inside the duct (n)
$L_{\mathrm{n}}(n=1\ldots9)$	Length of the duct (n)
$\sigma_{i,\mathrm{n}}(n=1,3,4,5,6,7)$	Heat transfer area inside the duct (n)
$\sigma_{e,\mathrm{n}}(n=1,3,4,5,6,7)$	External heat transfer area of the duct (n)
$\sigma_{i,\mathrm{n}}(n=2,9)$	Internal heat transfer area in the annular region (n) (see Figure 3)
$\sigma_{e,\mathrm{n}}(n=2,9)$	External heat transfer area in the annular region (n) (see Figure 3)
γ	Tilt angle of the bayonet heat exchanger
σ_V	Surface area of the mixer M

solution of the momentum equations is avoided, and the the problem is reduced to the solution of the energy equation. The temperature T_B of the pressurized water and vapour in the boiler is assumed as uniform and time-independent. The massive walls of the mixer M have been treated as a concentrated element, described by a unique temperature. This is a rough approximation; however it allows to fix our attention on the functional rather than on the morphological characteristics of the component. Order of magnitude evaluations suggested that the thermal impedance for the radial heat transfer inside the metallic ducts can be neglected.

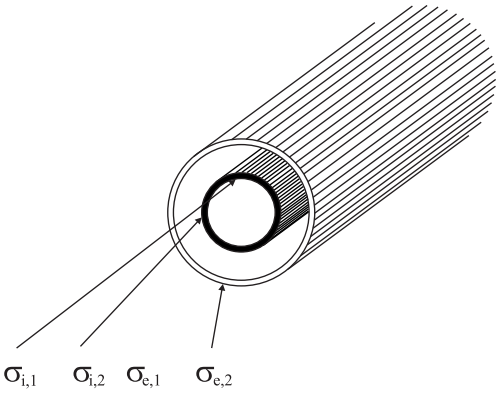

Figure 3. Cross section of the annular bayonet heat exchanger. The relevant surfaces for the heat transfer are labelled according to the indications of Table 1

2.2. The model equations

During the active phase the mass flow rates along the different elements of the circuit are related by the following conditions:

$$\dot{m}_2=\dot{m}_9=\dot{m}_4=\dot{m}_6,\quad \dot{m}_3=\dot{m}_5=\dot{m}_7,\quad \dot{m}_1=\dot{m}_2+\dot{m}_3. \tag{1}$$

The mass flow rate $\dot{m}_1$ is determined by the water demand, which in turn depends on the type of the coffee which is prepared (lower for an italian coffee and larger for an american coffee); the ratio $\dot{m}_2/\dot{m}_3$ is determined by the ratio of the hydraulic impedances in the channels C1 and C2, and can be regulated through the jigler J1.

The energy equations, for each element of the circuit, supplemented with the appropriate boundary conditions, are written as:

duct (1)

$$\frac{\partial T_1}{\partial t} + v_1 \frac{\partial T_1}{\partial x} = \frac{h_{1a} \pi D_{e,1}}{\rho c S_1} (T_a - T_1) + \alpha \frac{\partial^2 T_1}{\partial x^2}, \tag{2}$$

$$T_1(0) = T_i, \qquad T_1(L_1) = T_3(L_1) = T_2(L_1), \tag{3}$$

where in Equation (2) T_a and h_{1a} represent the fluid temperature in the annular volume and the heat transfer coefficient between the two fluids in the internal duct and in the annular region, respectively. The subscript a reads $a = 9$ when $0 \le x \le L_9$, and $a = 2$ when $x \ge L_9$. The parameters ρ, c, α represent the water density, specific heat and thermal diffusivity, respectively; v_1 is the fluid velocity in the duct (1);

duct (2)

$$\frac{\partial T_2}{\partial t} - v_2 \frac{\partial T_2}{\partial x} = \frac{h_{12} \pi D_{e,1}}{\rho c S_2} (T_1 - T_2) + \frac{h_{2B} \pi D_{e,2}}{\rho c S_2} (T_B - T_2) + \alpha \frac{\partial^2 T_2}{\partial x^2}, \tag{4}$$

$$T_2(L_9) = T_9(L_9); \qquad T_2(L_1) = T_3(L_1) = T_1(L_1), \tag{5}$$

where h_{2B} is the heat transfer coefficient between the fluid in the duct (2) and the water in the boiler;

duct (3)

$$\frac{\partial T_3}{\partial t} + v_3 \frac{\partial T_3}{\partial x} = \frac{h_{3B} \pi D_{e,3}}{\rho c S_3} (T_B - T_3) + \alpha \frac{\partial^2 T_3}{\partial x^2}, \tag{6}$$

$$T_3(L_1) = T_1(L_1) = T_2(L_1); \qquad T_3(L_1 + L_3) = T_5(0); \tag{7}$$

duct (4)

$$\frac{\partial T_4}{\partial t} + v_4 \frac{\partial T_4}{\partial x} = \frac{h_{4,ext} \pi D_{e,4}}{\rho c S_4} (T_{ext} - T_4) + \alpha \frac{\partial^2 T_4}{\partial x^2}, \tag{8}$$

where $h_{4,ext}$ is the heat transfer coefficient between the water flowing through the duct and the environment (air at local temperature T_{ext}).

$$T_4(0) = T_9(0), \qquad T_4(L_4) = T_6(0); \tag{9}$$

duct (5)

$$\frac{\partial T_5}{\partial t} + v_5 \frac{\partial T_5}{\partial x} = \frac{h_{5,ext} \pi D_{e,5}}{\rho c S_5} (T_{ext} - T_5) + \alpha \frac{\partial^2 T_5}{\partial x^2}, \tag{10}$$

$$T_5(0) = T_3(L_1 + L_3), \qquad T_5(L_5) = T_7(0); \tag{11}$$

duct (6)

$$\frac{\partial T_6}{\partial t} + v_6 \frac{\partial T_6}{\partial x} = \frac{h_{6,i} \pi D_{i,6}}{\rho c S_6} (T_{met} - T_6) + \alpha \frac{\partial^2 T_6}{\partial x^2}, \tag{12}$$

$$T_6(0) = T_4(L_4), \qquad \frac{\partial T_6(L_6)}{\partial x} = 0, \tag{13}$$

where T_{met} is the average temperature of the massive walls of the mixer M, and $h_{6,i}$ is the heat transfer coefficient between the fluid and the metallic walls;

duct (7)

$$\frac{\partial T_7}{\partial t} + v_7 \frac{\partial T_7}{\partial x} = \frac{h_{7,i} \pi D_{i,7}}{\rho c S_7} (T_{met} - T_7) + \alpha \frac{\partial^2 T_7}{\partial x^2}, \tag{14}$$

$$T_7(0) = T_5(L_5), \qquad \frac{\partial T_7(L_7)}{\partial x} = 0; \tag{15}$$

duct (9)

$$\frac{\partial T_9}{\partial t} - v_9 \frac{\partial T_9}{\partial x} = \frac{h_{19}\pi D_{e,1}}{\rho c S_9}(T_1 - T_9) + \frac{h_{9,ext}\pi D_{e,9}}{\rho c S_9}(T_{ext} - T_9) + \alpha \frac{\partial^2 T_9}{\partial x^2}, \tag{16}$$

$$T_9(0) = T_4(0), \qquad T_9(L_9) = T_2(L_9); \tag{17}$$

the mixer M

$$c_{met} M_{met} \frac{dT_{met}}{dt} = \int h_{7,i}\pi D_{i,7}(T_7 - T_{met})dx + \int h_{6,i}\pi D_{i,6}(T_6 - T_{met})dx + , + \int h_{met,air}(T_{air} - T_{met})d\sigma \tag{18}$$

where the subscript *met* relates to the thermophysical properties of metallic walls of the mixer, and T_{air} is the local temperature of the environment; $h_{met,air}$ is the heat transfer coefficient between the metallic walls of the mixer and the environment.

During the idle phase the model equations can be easily derived from the previous analysis, observing that now the valves V1 and V2 are closed, and the temperature gradient along the heat exchanger drives a free-convection flow due to the buoyancy forces. The flow along the ducts (2), (9), (4), (6) is inverted, and the mass flow rates are related by:

$$\dot{m}_1 = 0, \quad \dot{m}_3 = \dot{m}_5 = \dot{m}_7 = \dot{m}_6 = \dot{m}_4 = \dot{m}_9 = \dot{m}_2. \tag{19}$$

The overall flow rate must be determined evaluating the buoyancy forces and the overall hydraulic impedance of the circuit.

3. Thermohydraulic correlations

The heat transfer coefficient between the two fluids in counterflow, inside the heat exchanger, can be written as:

$$h_{12} = \frac{h_{11} \cdot h_{22}}{h_{11} + h_{22}}, \quad h_{19} = \frac{h_{11} \cdot h_{99}}{h_{11} + h_{99}}, \tag{20}$$

where h_{11} is the fluid-wall heat transfer coefficient at the wall $\sigma_{i,1}$; h_{22}, h_{99} represent the fluid-wall coefficients at the walls $\sigma_{e,1}$ (see Figure 3).

The flow in the annular region is always laminar; the Nusselt number for the heat transfer at the wall $\sigma_{e,1}$ is given by the correlations of Lundberg, McCuen e Reynolds [1] and its value is $Nu_{e,1} \sim 8$. In the internal duct (1) the flow may result to be either laminar or turbulent. In the first case the Nusselt number is $Nu_{i,1} \sim 4$; otherwise the Colburn equation [2] gives:

$$Nu_{i,1} = 0.023 Re^{0.8} Pr^{0.33}, \tag{21}$$

where Re and Pr represent the Reynolds and the Prandtl numbers, respectively, defined for the water at the local conditions as:

$$Re = \frac{\rho v D_{i,1}}{\mu}, \quad Pr = \frac{c\mu}{k}. \tag{22}$$

In the above equations μ, k represent the dynamic viscosity and the thermal conductivity of the water at the local conditions. The fluid-wall heat transfer coefficients are derived through:

$$h_{11} = \frac{k \cdot Nu_{i,1}}{D_{i,1}}, \quad h_{22} = \frac{k \cdot Nu_{e,1}}{D_{e,1}}, \quad h_{99} = \frac{k \cdot Nu_{e,1}}{D_{e,1}}. \tag{23}$$

In the annular duct (2) and in the clearance volume (3) the heat transfer at the external walls $\sigma_{e,2}$, $\sigma_{e,3}$ is essentially driven by natural convection. The nondimensional parameters which describe the process are the Grashof and Rayleigh numbers, defined as:

$$Gr = \frac{\rho^2 g cos(\gamma)\beta(T_B - T_\infty)(L_1 + L_3)^3}{\mu^2}, \quad Ra = Gr \cdot Pr, \tag{24}$$

where g is the body force due to gravity, β is the thermal expansion coefficient of the hot water, and T_∞ an average temperature of the water inside the annular and the clearance regions. In actual operating conditions we find $Gr \sim Ra \sim 10^{10}$; with these values the Nusselt number and the heat transfer coefficient at the walls $\sigma_{e,2}$, $\sigma_{e,3}$ are given by:

$$Nu_e = 0.555 \cdot Ra^{1/4}, \quad h_{e,2} = h_{e,3} = \frac{k \cdot Nu_e}{(L_1 + L_3)}. \tag{25}$$

The Nusselt number for the heat transfer between the bayonet heat exchanger and the pressurized fluid in the boiler can be determined through the correlations of Chen, Garner and Tien [3]; however the heat transfer coefficient is at least an order of magnitude larger than $h_{e,2}$, $h_{e,3}$, so we neglect the thermal impedances on this side of the exchanger.

For the heat dispersion towards the environment the Nusselt number is given by [4]:

$$Nu = \left\{ 0.6 + \frac{0.387 \cdot Ra^{1/6}}{[1 + (0.559/Pr)^{0.562}]^{0.296}} \right\}^2. \tag{26}$$

To estimate the mass flow rates during the active and idle phases we measured the the hydraulic impedances of the channels C1, C2 and of the whole circuit. The pressure jump ΔP is related to the mass flow rate through $\Delta P = \epsilon \cdot \dot{m}^2$, where the values of ϵ are $4.1 \cdot 10^6$, $3.0 \cdot 10^6$ and $7.1 \cdot 10^6$ (SI units) for the channels C1, C2 and for the whole circuit, respectively. These data allow to estimate the partition of the overall mass flow rate between the channels C1 and C2 during the active phase; the flow rate during the idle phase is determined observing that the driving pressure jump is:

$$\Delta P = \int_{asc} \rho[T(x)] g dx - \int_{disc} \rho[T(x)] g dx, \tag{27}$$

where ρ is the water density and in the R.H.S. integration is performed along the ascending and descending paths, respectively.

4. The numerical method and first numerical results

The model equations have been discretized with the finite difference method; an explicit Euler integration scheme was employed to advance the solution in time, and second order central differences were used for the spatial derivatives. To ensure an accurate resolution of the thermal field the grid spacing was selected as $\Delta x = 2.5 \cdot 10^{-3}$ m, and a time step $\Delta t = 2.0 \cdot 10^{-2}$ s was required for thermal stability. At each time step all the thermophysical properties of the system were updated.

To check the consistency of the model the equations have been solved using the values of the parameters specified in Table 2. In Figure 4 we show the temperature profile along the circuit, at the end of a long idle phase, when a stationary regime has been attained. The zero of the spatial coordinate on the horizontal axis is fixed at the inlet of the duct (9). We observe the sharp temperature rise along the heat exchanger until a maximum value of $T = 118^\circ$C; then the temperature decreases along the duct (5) and more sharply across the

Table 2. Values of the parameters utilized in the simulation

L_1 = 0.11 m	L_2 = 0.08 m
L_3 = 0.12 m	L_4 = 0.22 m
L_5 = 0.32 m	L_6 = 0.05 m
L_7 = 0.05 m	L_9 = 0.03 m
$D_{i,1}$ = 0.006 m	$D_{e,1}$ = 0.008 m
$D_{i,2}$ = 0.038 m	$D_{e,2}$ = 0.040 m
$D_{i,3}$ = 0.038 m	$D_{e,3}$ = 0.040 m
$D_{i,4}$ = 0.008 m	$D_{e,4}$ = 0.010 m
$D_{i,5}$ = 0.008 m	$D_{e,5}$ = 0.010 m
$D_{i,6}$ = 0.010 m	$D_{e,6}$ = 0.010 m
$D_{i,7}$ = 0.010 m	$D_{e,7}$ = 0.010 m
$D_{i,9}$ = 0.011 m	$D_{e,9}$ = 0.014 m
γ = $\pi/4$	$\dot{m}_1$ = 0.0035 Kg/s
T_i = 20 °C	T_{ext} = 50 °C
T_{air} = 35 °C	M_{met} = 2.7 Kg
t_a = 15 s	t_r = 10 s
startup time 4800 s	

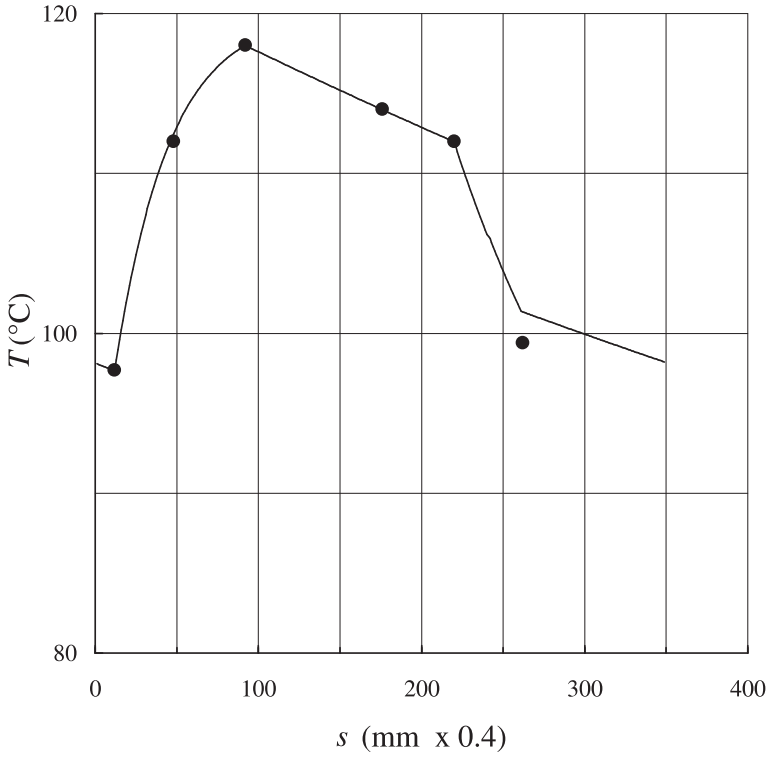

Figure 4. Temperature profile along the flow path, as predicted by the model (solid line) at the end of a long idle phase. The solid dots correspond to experimental data

mixer M. On the graph the solid dots represent the results of measures performed on the system. We can observe that the agreement between the predictions of the model and the

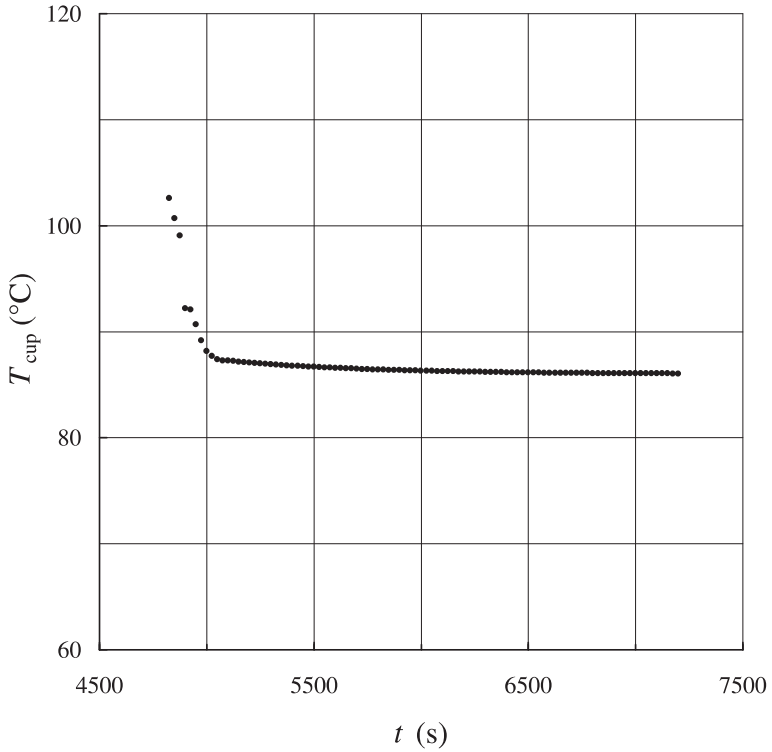

Figure 5. Average temperature of the water injected into the coffee filter during the active phase, after the startup time

actual temperature profile is quite satisfactory. In Figure 5 we represent as a function of time the evolution of the temperature of the water injected into the coffee filter, averaged along the active phase. We observe that after the startup of the coffee machine, the first few cups of coffee are delivered at a temperature well beyond the optimal range 85−95°C, but very soon a satisfactory regime is attained, with a cup temperature of 86°C.

5. Conclusions

We simulated the transient thermohydraulic behaviour of the heating circuit of an Espresso-Coffee Machine, in order to identify the best value of some design and operation parameters. The main characteristics of the heating process have been captured with a simple model, treating as far as possible the complex architepture of the machine through lumped parameters. The first numerical results show a good agreement between the prediction of the model and the experimental data.

References

[1] Lundberg R E, McCuen P A and Reynolds W C 1963 *Int. J. Heat Mass Transfer* **6** 495
[2] Kays W M and Perkins H C 1973 in *Handbook of Heat Transfer* ed. by Rohsenow W M and Hartnett J P, McGraw-Hill, New York
[3] Chen S L, Garner F M and Tien C L 1987 *Experimental Heat Transfer* **1** 93
[4] Bejan A 1993 *Heat Transfer* Wiley, New York